



PARAMETRIC STUDY OF VOLUTES FOR OPTIMAL CENTRIFUGAL FAN IMPELLERS

Ardit GJETA¹, Konrad BAMBERGER²,
Thomas CAROLUS², Andonaq LONDO¹

¹ *Mechanical Engineering Faculty, Polytechnic University of Tirana,
"Mother Tereza" Square, Nr. 4, Tirana, Albania*
*Institute for Fluid- and Thermodynamics, University of Siegen,
Paul-Bonatz-Str. 9-11, 57068 Siegen, Germany*

SUMMARY

European regulations set standards for energy-efficiency of fans, with increasing requirements in the near future. Many studies concerning centrifugal fans have investigated the impeller but to only a smaller extends the spiral casing, which may take up a substantial part of the fan's hydraulic loss. Hence, appropriate design of the fan volute has significant meaning to centrifugal fan performance. An automatized loop with RANS and data post-processing is set up for allowing a large number of parameter variations. The effect of volute angle, volute width and geometrical parameters related to the tongue and axial position of rotor, on total pressure loss and static pressure recovery coefficient are presented.

NOMENCLATURE

Indices

1	impeller inlet
2	impeller outlet (volute inlet)
3	volute outlet
<i>opt</i>	optimal
<i>min</i>	minimum
<i>max</i>	maximum
<i>t</i>	total
<i>ts</i>	total-to-static
<i>tt</i>	total-to-total

Greek Symbols

ϕ	flow coefficient
$\alpha = \arctan(c_m / c_u)$	alpha spiral angle
ψ	pressure coefficient
η	efficiency
ρ	air density

Abbreviations

CFD	Computational Fluid Dynamics
RANS	Reynolds Averaged Navier-Stokes
SST	Shear stress transport
FOAM	Field Operation And Manipulation

INTRODUCTION

A centrifugal fan that consists of an axial, an impeller and a spiral casing is widely used in industry as a typical piece of turbo-machinery that converts external mechanical energy into pressure and kinetic energy of the working fluid. An impeller is a mechanical device that supplies mechanical energy to the fluid and is a key component of the fan. Therefore, many studies have focused intensively on impellers. Fluids obtain energy from the impeller and it is discharged through the spiral casing. Currently, minimization of energy loss is dependent on the characteristics of the spiral casing. Research on the spiral casing has drawn relatively little attention, but in order to improve the performance of centrifugal fans to a higher level, study of the characteristics of the spiral casing is absolutely needed.

Industrial fans are subject to EU energy labeling and Ecodesign requirements. By using more efficient industrial fans, Europe will save 28 TWh and avoid 11 million tones of CO₂ emissions annually by 2020. Ecodesign requirements for industrial fans are mandatory for all manufacturers and suppliers wishing to sell their products in the EU. These requirements cover product information and efficiency [1].

METHODOLOGY

Volute shape design method

The spiral housing in radial fans has the task of collecting the fluid in a low-loss manner and converting kinetic energy into static pressure. Constant circulation method [2] is a method to draw spiral case based on that the velocity circulation is a constant $r \cdot c_u = const$. In practice this rule is valid with the restriction that one spiral must be so far displaced from the impeller that deflections conditioned by the consideration of a finite number of blades can be ignored. This rule constitutes the basis for the dimensioning of a volute for the case where friction has been ignored. The velocity c at an arbitrary place can be calculated from its components c_m and c_u , $r \cdot c_u = r_2 \cdot c_{u2} \rightarrow c_u = c_{u2} \cdot (r_2 / r)$. From the condition that the same volume flow must flow (continuity equation) through all the streamline in volute it gives the relationship, $\dot{V} = 2\pi \cdot r_2 \cdot b_2 \cdot c_{m2} = 2\pi \cdot r \cdot B \cdot c_m$, from which follows $r_2 \cdot b_2 \cdot c_{m2} = r \cdot B \cdot c_m$, from this we obtain the following inclination α of the streamlines:

$$\tan(\alpha) = \frac{c_m}{c_u} = \frac{c_{m2}}{c_{u2}} \frac{b_2}{B} \quad (1)$$

Because we obtain the boundary of the volute from the streamline, again it yields, $\tan(\alpha) = \frac{dr}{rd\varphi}$

$$\frac{dr}{r} = d\varphi \tan(\alpha) = d\varphi \tan(\alpha_2) \frac{b_2}{B} \quad (2)$$

The solution states,

$$\ln \frac{r}{r_2} = \varphi \tan(\alpha_2) \frac{b_2}{B} = \varphi \frac{c_{m2}}{c_{u2}} \frac{b_2}{B} \quad (3)$$

Accordingly, the trajectory of fluid particles in the volute is as follows (Carolus 2013) [3]

$$r_{(\varphi)} = r_2 e^{\varphi \tan(\alpha)} = r_2 e^{\varphi \tan(\alpha_2) \frac{b_2}{B}} \quad (4)$$

$r_{(\varphi)}$, is the radius of the volute at an angle φ ,

r_2 , is the outer radius of impeller that is equal to 150mm in this case

α , is the angle that absolute velocity vector makes with the peripheral direction $\tan(\alpha) = c_m / c_u$.

b_2 , width of outlet impeller

B , width of volute

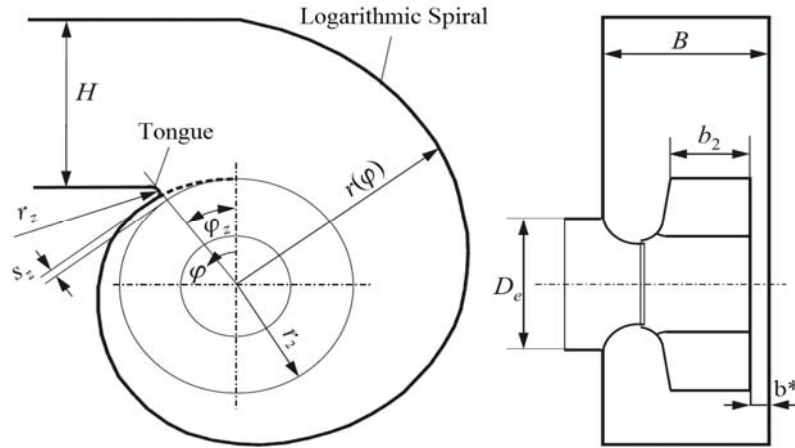


Figure 1: Geometry parameters of spiral casing (Carolus 2013) [3]

In this parametric study, is shown the effect of: spiral alpha angle α , tongue angle ϕ_z , tongue radius r_z , volute width scale B/b_2 , the position of impeller and volute inlet profile velocity on the performance of the centrifugal fan by using open source CFD software OpenFOAM. A qualitative understanding on the effects of those parameters will enable performance of a real product to be improved.

Optimal impeller

Starting point are optimal impellers for the whole range of specific speeds. Following a current and nearly finished study on aerodynamic optimization of centrifugal fan impellers using CFD-trained meta-models [4], where a method for optimization of impellers of the whole class of centrifugal fans has been developed. For the first simulations it is accepted one optimized impeller (VAL_1) with the design flow coefficient $\phi = 0.12$, which correspond to flow rate of $0.4m^3/s$, since the diameter of the impeller is $0.3m$ and the rotational speed is $3000rpm$. The detailed flow field at the impeller's outlet from preceding RANS simulations is used as boundary conditions for an RANS of the flow in the volutes.

Performance of the volute

The overall performance of the volute is affected mainly by the following geometric parameters (Ayder 1993) [5]: area of the cross-section, shape of the cross-section, radial location of the cross-section, location of the impeller and tongue geometry.

The overall performance of the volute can be analyzed by using:

Total pressure loss coefficient of volute:

$$K_p = \frac{P_{t2} - P_{t3}}{P_{t2} - P_2} = \frac{P_{t2} - P_{t3}}{\frac{\rho}{2} c_2^2} \quad (5)$$

K_p , is defined as the ratio between the total pressure losses in volute to the dynamic pressure at the impeller exit.

Static pressure recovery coefficient of volute:

$$C_p = \frac{P_3 - P_2}{P_{t2} - P_2} = \frac{P_3 - P_2}{\frac{\rho}{2} c_2^2} \quad (6)$$

C_p , is defined as the ratio between the static pressure recovered in the volute to the dynamic pressure at the impeller exit.

Total Efficiency of volute

$$\eta_t = \frac{P_{t3}}{P_{t2}} \quad (7)$$

From equation (5, 6) becomes:

$$C_p = 1 - K_p - \frac{c_3^2}{c_2^2} \quad (8)$$

$\frac{c_3^2}{c_2^2}$, is the ratio of volute outlet/inlet kinetic energy.

Total to static pressure of complete machine:

$$\Delta p_{ts} = P_{t3} - P_{t1} - \frac{\rho}{2} c_3^2 = (P_3 - P_2) + (P_2 - P_1) - \frac{\rho}{2} c_1^2 = C_p \frac{\rho}{2} c_2^2 + R \Delta p_{tt} - \frac{\rho}{2} c_1^2, \Delta p_{tt} = P_{t3} - P_{t1} \quad (9)$$

$R = \frac{P_2 - P_1}{P_{t2} - P_{t1}}$, is degree of reaction of blade cascade (i.e. impeller)

Maximizing Δp_{ts} of a complete fan requires:

- Maximizing degree of reaction R of blade cascade, which is function of impeller design, accepted as a fixed parameter.
- Finding $c_{3,opt}$, $K_{p,opt} = K_{p,min}$, $C_{p,opt} = C_{p,max}$ from CFD as a function of all geometric parameters of volute (alpha spiral angle, width scale, tongue angle, tongue radius, etc).

Numerical analysis

Numerical simulations were performed using the Open Source CFD software, OpenFOAM v3.0.x [6]. Three-dimensional, incompressible, steady-state flow computations were carried out at the University of Siegen. This solves discretized forms of the Reynolds-averaged Navier–Stokes equations for turbulent flow using the finite volume method (Ferziger, Perić 2002) [7]. The unstructured grid solution procedure is based on a variant of the SIMPLE pressure correction technique (Patankar 1980) [8]. The iterative solution was deemed to be converged when the normalized absolute error over the mesh had reduced to 10^{-5} for each variable. OpenFOAM supports the standard $k-\omega$ model by Wilcox (1998) [9], and Menter's SST $k-\omega$ model (1994)[10]. The $k-\omega$ SST turbulence model was employed for these calculations, with near-wall conditions supplied by the 'wall function' conditions of Launder and Spalding, 1974 [11]. $k-\omega$ models have gained popularity mainly because can be integrated to the wall without using any damping functions. This is the most widely adopted turbulence model in the aerospace and turbo-machinery communities.

Boundary and initial conditions

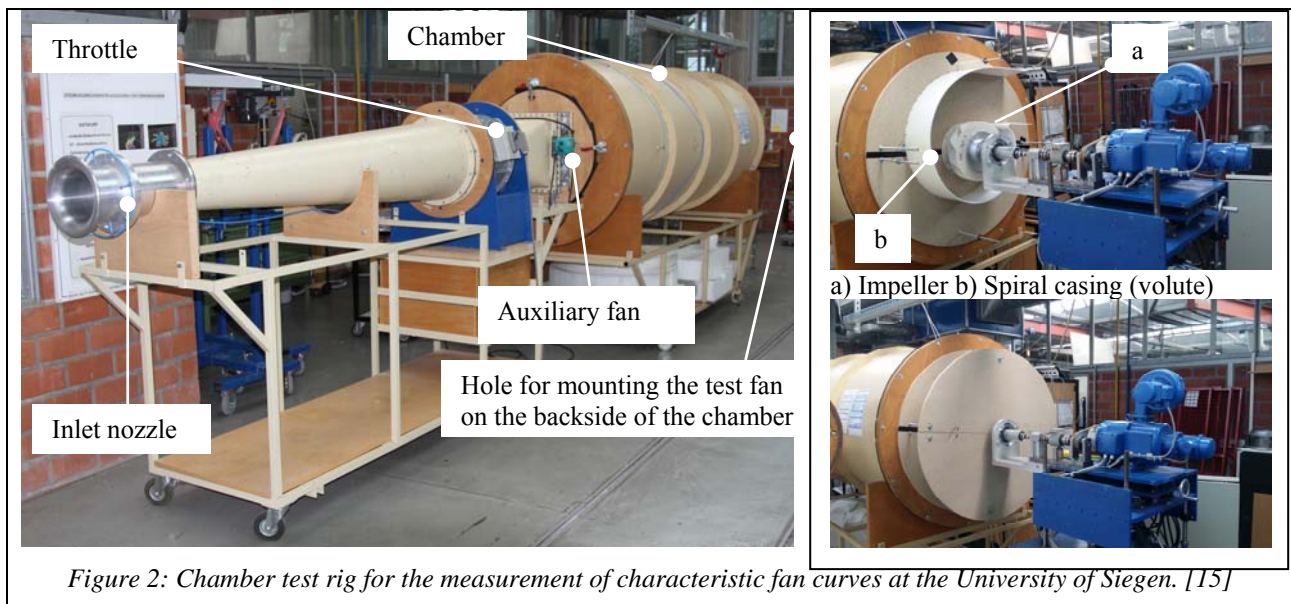
The inflow boundary conditions were based on known flow rates and the flow direction. Uniform velocity profiles were prescribed at the volute inlet (fan impeller outlet) by specifying radial and tangential velocity components separately (axial velocity is neglected). The front and back side of the impeller as the rotating wall, the other parts wall with no slip condition and for the outlet ambient pressure is used. Turbulent kinetic energy is $k = 3 \cdot m^2 s^{-2}$, and the specific turbulence dissipation rate is $\omega = 4000 \cdot s^{-1}$.

The geometry of volutes is generated from MATLAB as a stereolithography (.stl file), than cfMesh v1.1.2 software is used to create mesh. Grid resolution is made according

to $y+$ value ($30 < y+ < 200$) and the number of cells varies from 250.000 for the compact volutes to 500.000 cells.

Experimental set-up

All experimental investigations are conducted at the chamber test rig of the University of Siegen. The layout is in accordance with EN ISO 5801:2009 [12]. The measuring uncertainty was estimated by Hensel [13] and Winkler [14] and amounts to 1% regarding φ , 0.5% regarding ψ_{ts} , and 2% regarding η_{ts} . The test rig is shown in Figure 2. Air is sucked in through the test rig inflow nozzle at which the static pressure is measured. The air then passes an auxiliary fan and a throttle. These two devices are used to vary the flow rate in the interval required for the characteristic curve. Downstream of the throttle, the air is decelerated in a large chamber. The chamber has four small holes where the pressure is taken. Due to the extremely slow velocity in the chamber, the static pressure measured is assumed to be equal to the total pressure. At the backside of the chamber, the test fan is introduced a short duct with an inlet nozzle. The fan faces the chamber with its suction side and is driven by an electric motor. The driving power is determined by measuring the torque and the rotational speed of the shaft driving the fan [15].



RESULTS

Effect of spiral alpha angle

The first simulations were made with constant tongue angle $\phi_z = 45^\circ$ and tongue radius $r_z / D_2 = 5\%$, with the simplified geometry of impeller, and the position of impeller in the middle of volute.

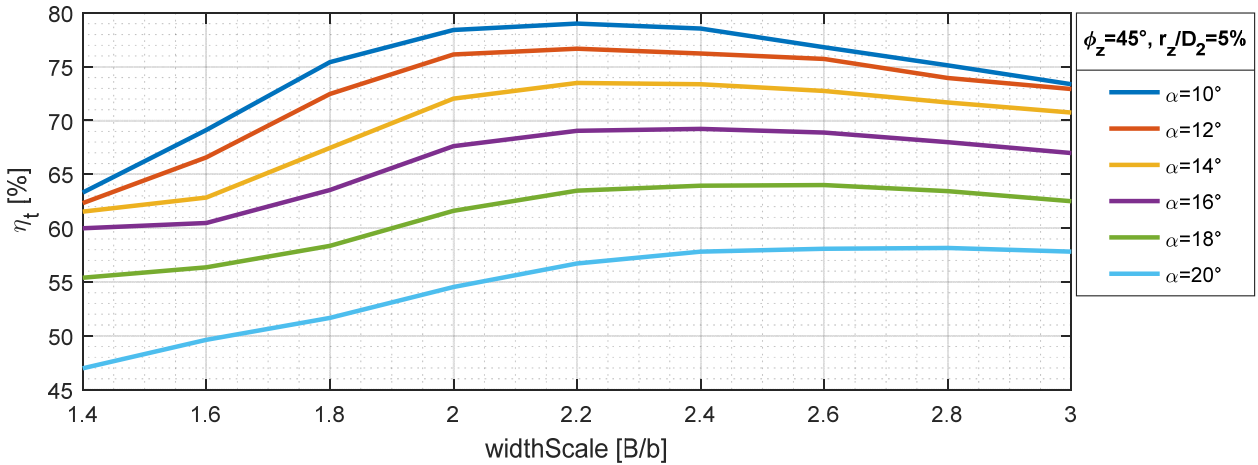


Figure 3: Comparison total efficiency of volutes for different alpha angle function of width scale B/b

Total to total efficiency of volutes as a function of width scale is shown in Figure 3 for each of alpha spiral angle. As a result of the different values of alpha angles as it is shown on the graph, the maximum efficiency is taken for smaller values of alpha, corresponding to a compact volute. Which in the cases of bigger ones consist at lower efficiency, due to the surface of walls.

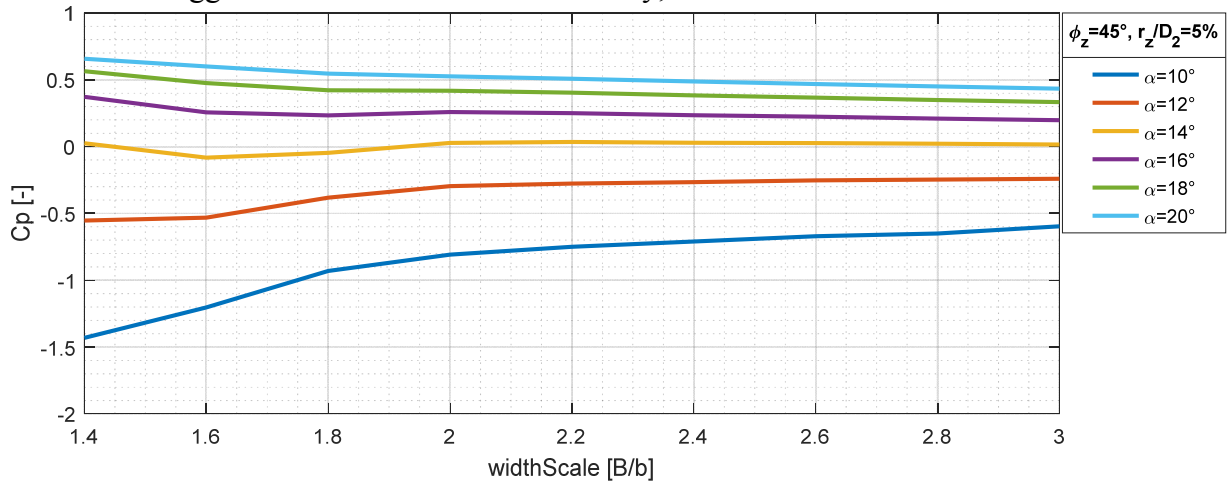


Figure 4: Static pressure recovery coefficient of volutes for different alpha angle function of width scale $\frac{B}{b}$.

Static pressure recovery coefficient as a function of width scale is shown in Figure 4. For higher value of alpha spiral angle consist at maximum value of static pressure recovery coefficient. It is observed that with the increase of width scale for the smaller alpha spiral angle respectively for alpha 10°, 12° and 14°, results in higher value of static pressure recovery coefficient, the situation is different for alpha 16°, 18° and 20°.

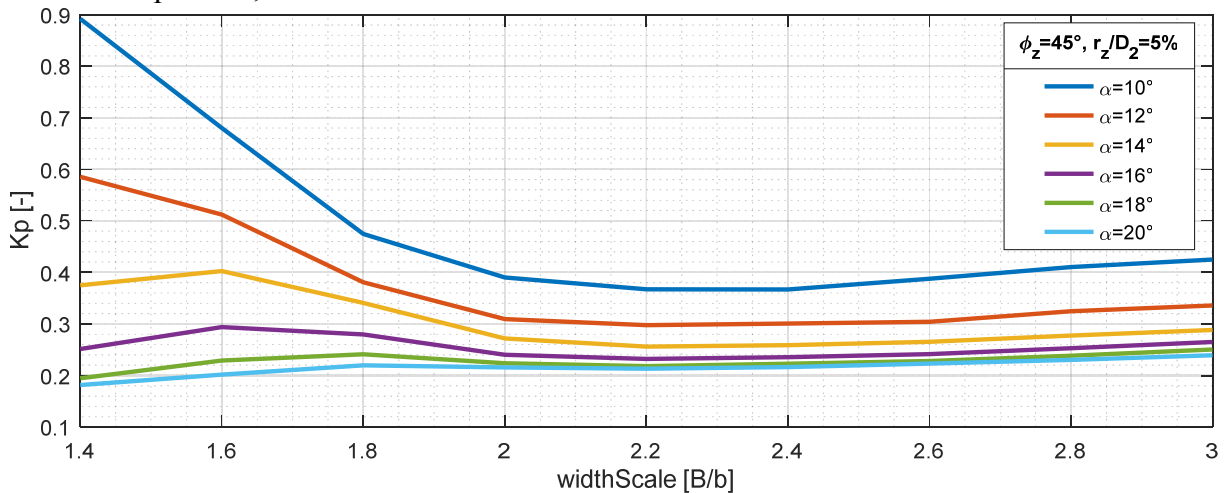


Figure 5: Total pressure loss coefficient of volutes for different alpha angle function of width scale $\frac{B}{b}$.

Analyzing the total pressure loss coefficient in figure 5, the variance is opposite to the pressure recovery coefficient and the optimal values are obtained in the values of the width scale $B/b=2, 2.2, 2.4$ and 2.6 .

Effect of tongue angle

Simulations are executed accepting constant alpha spiral angle $\alpha = 10^\circ$ and tongue radius $\frac{r_z}{D_2} = 5\%$

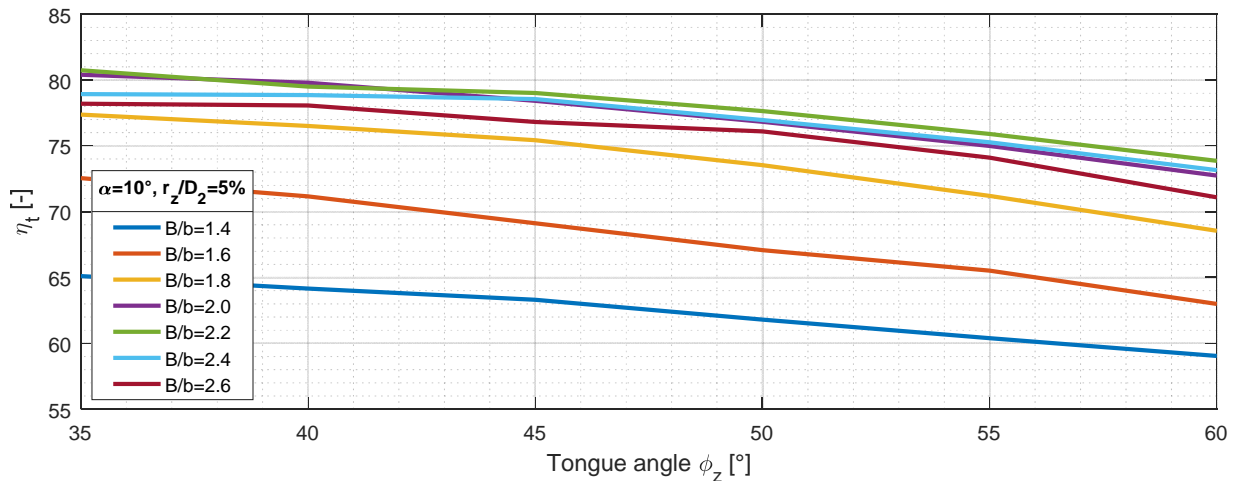


Figure 6: Total efficiency of volutes for different width scale $\frac{B}{b}$ function of tongue angle ϕ_z .

As it shown in graph of the figure 6 for lower values of tongue angle results on higher value of efficiency, which is absolutely true for all the range of width scales. From the graph above, the maximum efficiency value corresponds to width scale $B/b=2.2$, following $2.4, 2.0$ and 2.6 . The minimum efficiency value corresponds to width scale $B/b=1.4$, following 1.6 and 1.8 , which consist the same as in the figure 3. It is recommend excluding values of tongue angle below 35° , because of the effect to the clearance gap s_z , and the value should be according to the recommendation value [16]. The maximum efficiency is achieved for tongue angle 35° .

The simulations are carried out with constant width scale $B/b = 2.2$ and tongue radius $r_z / D_2 = 5\%$

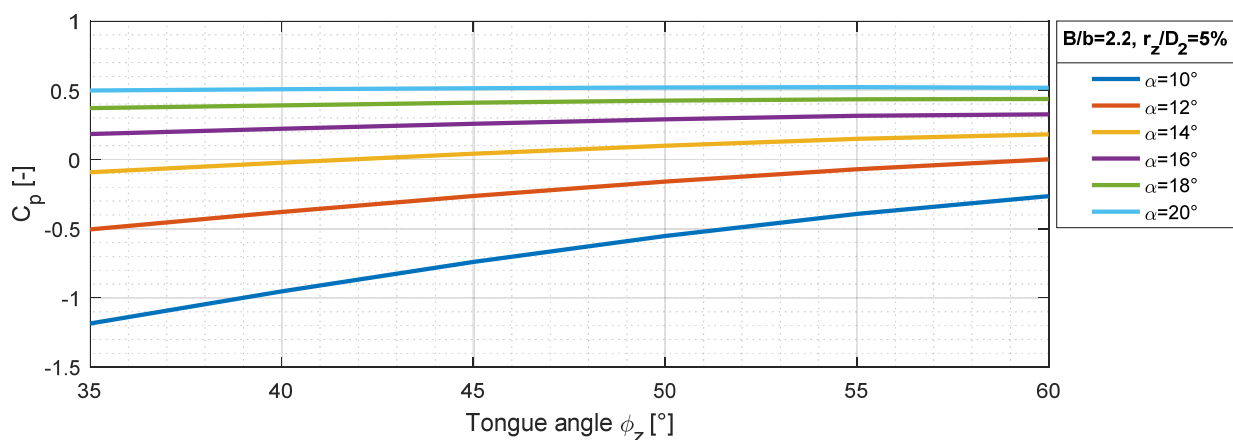


Figure 7: Static pressure recovery coefficient of volutes for different alpha angle function of tongue angle ϕ_z .

As it is shown from the figure 7 for smaller spiral alpha angle ($10^\circ, 12^\circ$ and 14°), by increasing tongue angle, results on higher possible value of static pressure recovery coefficient. In the cases of

alpha angle (16°, 18° and 20°) variance of the tongue angle, does not effect on the static pressure recovery coefficient, which is nearly constant.

Effect of tongue radius

These simulations were made with constant width scale $B/b=1.6$ and tongue angle $\phi_z = 35^\circ$. By increasing the radius of tongue for spiral alpha angle 10°,12° the efficiency is slightly increased, while for alpha 14°,16°,18° and 20° the efficiency is slightly decreased. Finally, it is important to notice, for alpha 10°, 12° the maximum efficiency is achieved for the radius of tongue 5%, and the situation is different for bigger volutes.

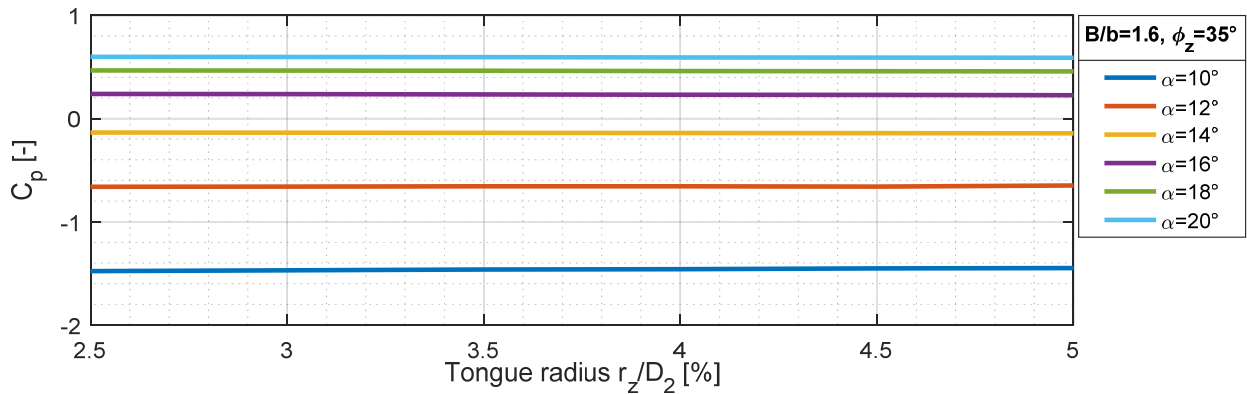


Figure 8: Static pressure recovery coefficient of volutes for different alpha angle function of tongue radius $\frac{r_z}{D_2}$.

As it is shown by the graph 8, radius of volute tongue has no considerable effect on the static pressure recovery coefficient.

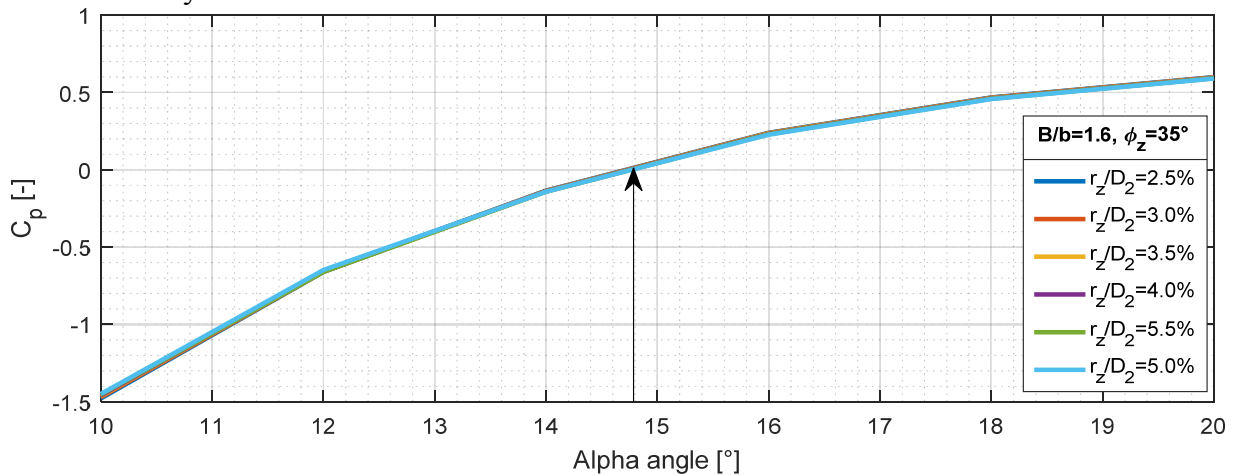


Figure 9: Static pressure recovery coefficient of volutes for different tongue radius $\frac{r_z}{D_2}$ function of alpha angle .

As it is shown from the graph 9 there are no considerable changes on the value of C_p , but it is observed that for alpha spiral angle over 14.8°, result on positive value of static pressure recovery coefficient

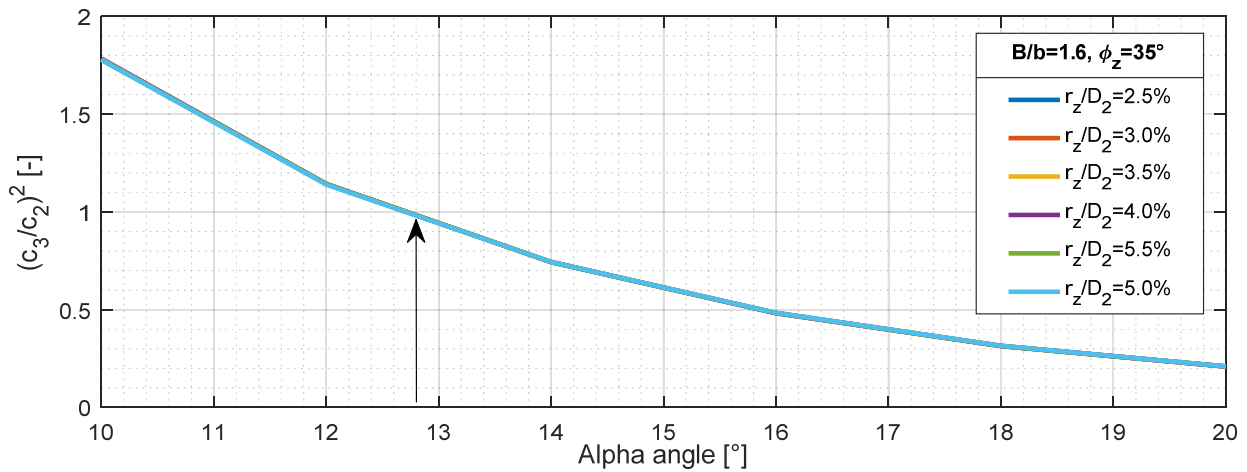


Figure 10: Outlet/inlet ratio of kinetic energy of volutes for different tongue radius $\frac{r_z}{D_2}$ function of alpha angle .

From graph 10 for alpha over 12.8° the ratio of kinetic energy is below value 1.

Effect of inlet velocity profile

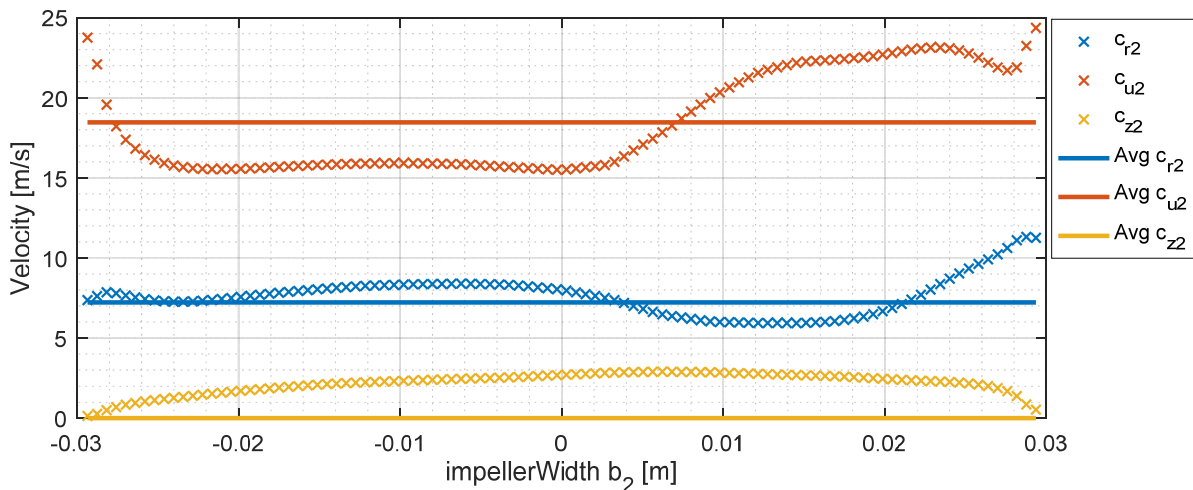


Figure 11: Velocity profile from the impeller CFD results and the average value [4].

From the CFD results of impeller [4], the velocity profile for each of velocity components (c_{u2} , c_{r2} , c_{z2}) are shown in the figure 11, supposing the same velocity profile along the width of impeller and checking the differences of simulation results with the average values of velocity.

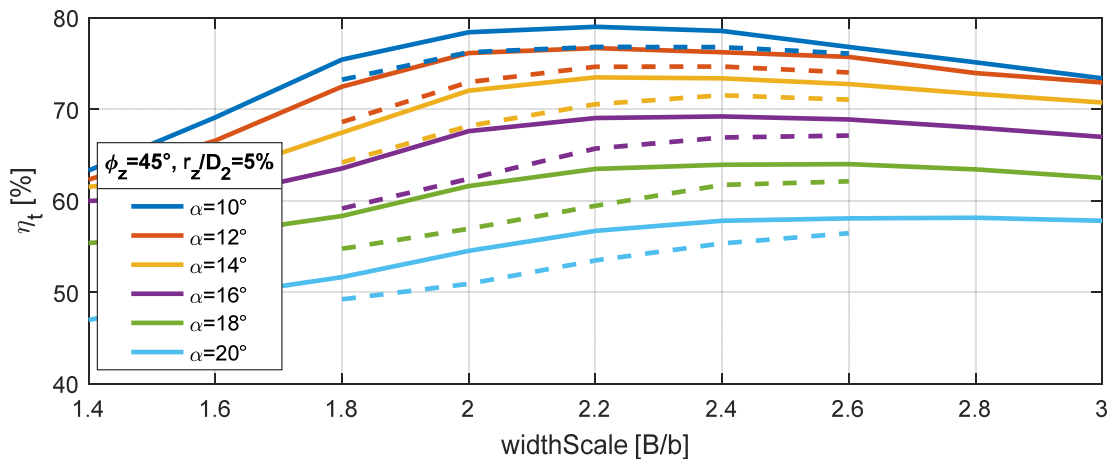


Figure 12: Comparison efficiency of volute with uniform and non uniform inlet velocity

From the figure 12 it is illustrated the comparison in efficiency for real velocity outlet profile of the impeller which corresponds to a lower value of efficiency.

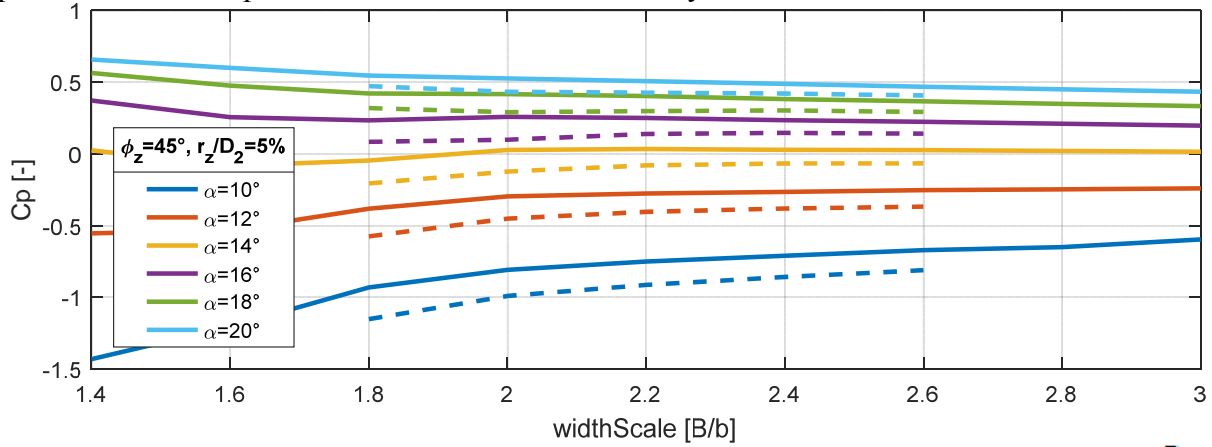


Figure 13: Static pressure recovery coefficient of volutes for different alpha angle function of width scale $\frac{B}{b}$.

The velocity profile has an important effect on static pressure recovery and total pressure loss coefficient, where for each of the cases, a lower value of C_p and a higher value of K_p is observed.

Effect of impeller position

These simulations were made with constant alpha angle $\alpha = 10^\circ$, tongue angle $\phi_z = 45^\circ$ and tongue radius $r_z / D_2 = 5\%$

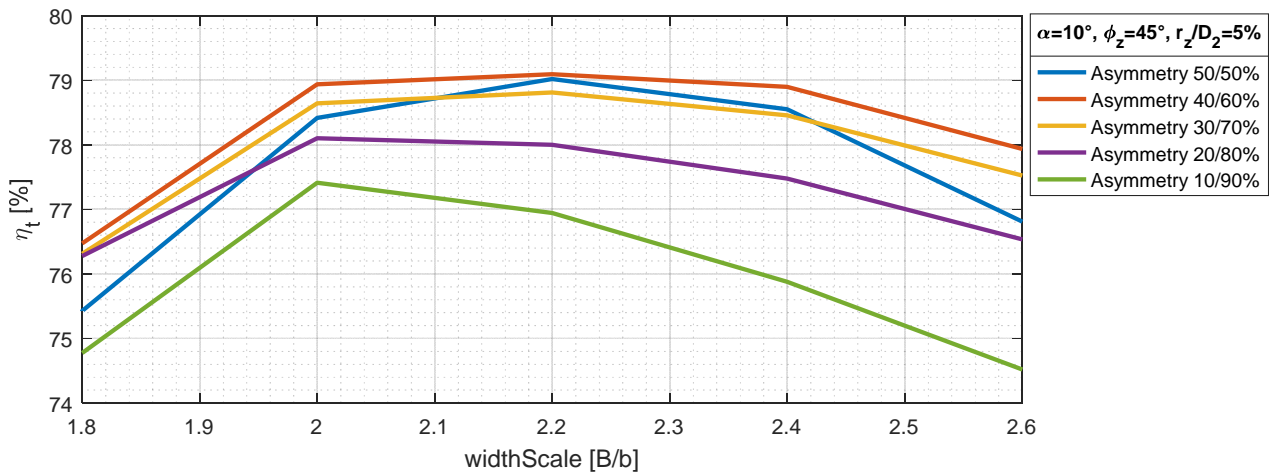


Figure 14: Total efficiency of volutes for different position of impeller

From the figure 14 it is illustrated the comparison in efficiency for different position of impeller, as it is shown, the maximum efficiency is achieved if the impeller is in asymmetry of 40% of the volutes, and the minimum efficiency achieved is if the impeller is in 10% of the volutes.

Validation of the CFD results

Based on the experimental data, total to static pressure Δp_{ts} and the total to static efficiency η_{ts} of the fan can be calculated from the following equation:

Total to static pressure of fan

$$\Delta p_{ts} = p_3 - p_{t1} = (p_3 - p_2) + (p_2 - p_{t1}) = C_p \frac{\rho}{2} c_2^2 + \Delta p_{ts,imp} \quad (10)$$

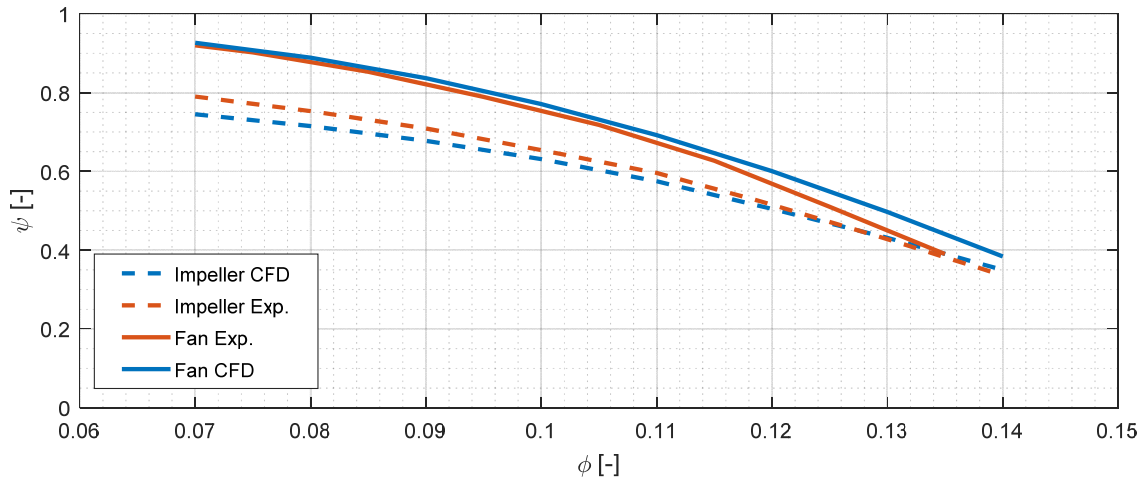


Figure 15: Comparison results from experiments and CFD for impeller and for the complete fan.

As it is shown from the figure 15, for small value of flow rate, the results of CFD and experiments can be fitted well for the impeller and the complete fan, also. For maximum value of flow rate, there is a difference but not higher than 4.4%.

Total to static efficiency of fan

$$\eta_{ts} = \frac{\Delta p_{ts} \dot{V}}{P_{shaft}} = \frac{C_p \frac{\rho}{2} c_2^2 \dot{V}}{P_{shaft}} + \frac{\Delta p_{ts,imp} \dot{V}}{P_{shaft}} = \frac{C_p \frac{\rho}{2} c_2^2 \dot{V}}{P_{shaft}} + \eta_{ts,imp} \quad (11)$$

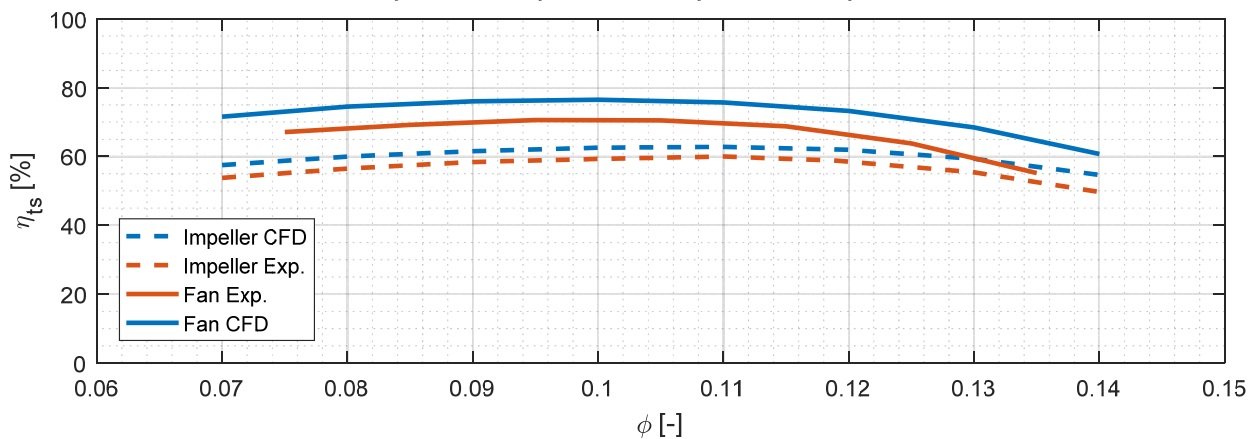


Figure 16: Comparison total to static efficiency from experiments and CFD results for impeller and for the complete fan.

As a conclusion, based on the CFD results, the efficiency is greater compared to the experimental data. As it shown in the figure 16 the curves of the efficiency have the same law performance, but values of the fan CFD results are 6 % over the experimental curve. The effect of recirculation flow inside the volute and impeller is not considered in our CFD simulation, this is related with safety distance between the impeller and the inlet nozzle. From the previous study on the impeller, the recirculation flow rate is between 7-8%.

CONCLUSIONS

This paper discusses the influence of spiral casing design geometric parameters on overall performance for centrifugal fan. Steady state CFD simulations have been conducted in order to study the characteristics of different volute configurations. The design was developed by systematically modifying the geometric parameters and predicting the internal three-dimensional flow structure using an open source CFD toolbox. The static pressure recovery coefficients as well as total pressure loss coefficient variations in the casing are investigated. The following conclusions deduced from the CFD simulation results are:

Smaller volutes have higher efficiency, but there is no pressure recovery. The reduction of the radius of the spiral casing cross-section causes an acceleration of the fluid and partially destroys the static pressure rise achieved in the diffuser.

The internal flow distribution could be improved by reducing the tongue angle, but it is needed to ensure the clearance gap s_z between volute tongue and impeller. While the radius of tongue has no effect on the C_p and K_p . Positive static pressure recovery can be reached for alpha spiral angle over 14.8° and the ratio of kinetic energy can be lower than 1 for alpha spiral angle over 12.8° .

The velocity profile of the outlet impeller effect in the negative way on the efficiency, C_p , K_p , etc, and should be considered on the next simulations.

The work of this paper represents a beginning for improving the volute design and needs to be continued and to be further improved in order to lead to better performance of centrifugal fans. The CFD simulations of the complete fan potentially will absolutely collect more information in the interaction of volute in the impeller and vice versa. Moreover, future researches should try to diminish the deviation between the numerical results (CFD) and the experimental data.

ACKNOWLEDGEMENT

The experimental work presented in this paper has been carried out at Institute for Fluid and Thermodynamics, University of Siegen, Germany. All support from the staff members is gratefully acknowledged.

BIBLIOGRAPHY

- [1] COMMISSION REGULATION (EU) No 327/2011 of “*Implementing Directive 2009/125/EC of the European Parliament and of the Council with regard to Ecodesign requirements for fans driven by motors with an electric input power between 125 W and 500 kW*”, **30 March 2011**
- [2] Eck, B.: “*Fans, Design and operation of centrifugal, axial-flow and cross-flow fans*”. Pergamon Press, **1973**
- [3] Carolus, Th.: “*Ventilatoren*”, Springer, **2013**
- [4] Bamberger K., Belz J., Carolus Th., Nelles O. “*Aerodynamic Optimization of Centrifugal Fans Using CFD-Trained Meta-Models*”. International Symposium on Transport Phenomena and Dynamics of Rotating Machinery (ISROMAC), Hawaii, Honolulu, April 10-15, **2016**
- [5] E. Ayder R. Van den Braembussche: “*Experimental and Theoretical Analysis of the Flow in a Centrifugal Compressor Volute*”, **1993**
- [6] OpenFOAM, “*The Open Source CFD Toolbox, User Guide*” Version 3.0.1, **2015**
- [7] Ferziger, Joel H.; Perić, M.: “*Computational methods for fluid dynamics*”. 3rd, rev. ed. Berlin, London: Springer, **2002**

- [8] Patankar, S. V.: “*Numerical Heat Transfer and Fluid Flow*”, Hemisphere Publishing Corporation, **1980**
- [9] Wilcox David C.: “*Turbulence Modeling for CFD*”, **1994**
- [10] Menter, F. R. & Esch, T. “*Elements of Industrial Heat Transfer Prediction*”. 16th Brazilian Congress of Mechanical Engineering (COBEM), **2001**
- [11] Launder, B. E. and Spalding, D. B. “*The numerical computation of turbulent flow*”. Computer Methods in Applied Mechanics and Engineering 3, 269-289, **1974**
- [12] ISO 5801:2009, “*Industrial fans -- Performance testing using standardized airways*”, **2009**
- [13] Hensel, K.: “*Konzeption eines Ventilatorprüfstandes nach DIN 24163*”, Final thesis no.A93030003, University of Siegen, Siegen. **1993**
- [14] Winkler, J.: “*Investigation of Trailing-Edge-Blowing on Airfoils for Turbomachinery Broad-band Noise Reduction*”, PhD thesis, University of Siegen, Siegen. **2011**
- [15] Bamberger K., Carolus Th., Haas M.,” *Optimization of Low-Pressure Axial Fans and Effect of Subsequent Geometrical modifications* “, **2015**
- [16] Bommers, L., Fricke, J., Grundmann, R.: ” *Ventilatoren* “. Vulkan-Verlag, Essen, **2003**